BIONANOCOMPOSITE FILM OF KAPPA-CARRAGEENAN / NANOTUBE CLAY: GROWTH OF HYDROXYL APATITE AND MODEL DRUG RELEASE

I. F. WAHAB[a, b], S. I. ABD RAZAK[a, b*]
[a]IJN-UTM Cardiovascular Engineering Centre, Universiti Teknologi Malaysia, 81310 Skudai, Johor, Malaysia
[b]Medical Devices and Technology Group, Faculty of Biosciences and Medical Engineering, Universiti Teknologi Malaysia, 81310 Skudai, Johor, Malaysia

This paper reports for the first time the reinforcement of kappa-carrageenan (κCRG) with clay of halloysite nanotubes (HNT) as potential biomedical materials. The bionanocomposite films (κCRG/HNT) were successfully prepared having optimum tensile properties at 3 wt% of HNT. Morphological and surface analysis of the nanocomposite revealed excellent film formation and increased in surface roughness. Immersion of the film in simulated body fluid for 7 days resulted in the growth of hydroxyl apatite particles with Ca/P ratio of 1.68. This is a good indication of bioactivity for possible template in bone tissue engineering. Swelling and methylene blue release experiments indicated possible drug delivery applications due to the stability of the κCRG matrix up to more than 20 days and delayed release of the model drug, respectively. This bioresource nanocomposite film has potential as a suitable biomedical material that requires mechanical integrity, bioactivity and drug releasing.

1. Introduction

Carrageenans (CRGs) are polysaccharides derived from red seaweeds that are well known in the food industry. They are highly soluble in water and very popular gelling agents [1]. Research on CRG hydrogels in biomedical and pharmaceuticals are still ongoing [2], mainly to create a more sustained drug release system through oral administration [3-5] and the production of semi-synthetic antibiotic [6-8]. Kappa-carrageenan (κCRG) is one of the sub-types of CRGs that contained one unit in sulphate group, thus making it an easy film forming substance [9, 10]. Even though κCRG films have been extensively explored particularly in food packaging applications [11-13], recent studies have shown that κCRG films exhibit potentials to be formulated as dressings for drug delivery to wounds [14] and possible enhanced bioactivity for bone tissue engineering [15]. Moreover the resemblance of κCRG chemical structure to glycosaminoglycans that compose the extracellular matrix of mamallian tissue opens up many possible functions as biomedical materials [16-17].

Therefore there is a need to explore even further the potential use of κCRG based films in these fields. The advantages of κCRG compared to synthetic polymers are due to their renewability and sustainability. Even so, their applications tend to be limited by their relative inherently low mechanical properties [18, 19]. Reinforcing the κCRG films with nanomaterials can be one of the strategies to solve this issue. Though several reinforcing agents have been added into κCRG film such as layered clays [20], carbon nanotubes (CNTs) [21], nanocellulose [11], nanosized silica [22] and gold nanoparticles [23], their methods were cumbersome and were not

---

[*]Correspondence: saifulizwan@utm.my

directed toward biomedical applications. Thus a more cost effective, biofriendly and biocompatible reinforcing filler is needed.

Halloysite nanotubes (HNT) are natural-occurring tubular clay material with many interesting characteristics. Their tubular structure and high surface area are comparable to that of CNTs. HNTs are at an advantage because they are nontoxic, biocompatible, cheaper and easier to disperse in polymeric matrix [24]. Reinforcing polymers with HNT have shown significant mechanical improvement [25]. Besides being used as reinforcing filler, lumen of HNT provide excellent site for the loading and release of active agents. Due to their unique inner and outer surface features, HNT have been investigated in drug delivery applications [26,27]. In-vitro bioactivity immersion in simulated body fluid (SBF) is a useful method because its composition is very close to that human blood plasma. Biomimetic immersion in SBF can be considered a moderate way to grow an apatite layer on a substrate. Recent report has shown that HNT promote the growth of hydroxyl apatite (HA) particle of the matrix composite after immersion in SBF [28].

Up to date, reinforcing κCRG film with nanotubes clay is an unexplored strategy. To the best of our knowledge this is the first attempt of such modifications. Hence it is envisioned that the κCRG/HNT nanocomposite films could be mechanically reinforced and at the same time showing enhanced HA forming ability and delay drug releasing properties. Thus the aim of this study is to develop nanocomposite films of κCRG/HNT with enhanced mechanical properties which have potentials to be used in biomedical applications. We examined the tensile properties, morphological and structural features of the nanocomposite films. Potential uses of the films as hydroxyl apatite growth template and drug delivery material were investigated as well.

2. Experimental

2.1. Preparation of Nanocomposite Films

Nanocomposite films of κCRG/HNT were prepared according to the following procedures. 2 grams of κCRG (Sigma) was dissolved in 250 ml of deionized water for about an hour. In the meantime a predetermined amount of HNT powder (Sigma) was suspended in deionized water followed by vigorous stirring. Both solutions were mixed by transferring the κCRG solution into the HNT containing suspension. 40 w/w% of glycerol (Merck) to κCRG was added with continued stirring for 2 hours. The temperature was elevated to 65°C for 10 minutes. The mixed solution was then cooled down to 45°C and was transferred into a mould and further dried at 45°C. Following above procedure, κCRG/HNT nanocomposites with required filler loading (1, 2, 3, and 4 w/w% to CRG content) were prepared. As for the model drug for the release experiments, methylene blue (MB) solution was added into the suspended HNT solution before the mixing with κCRG solution. Neat κCRG films were prepared for comparison purposes.

2.2. Characterizations

The tensile tests were performed using a computer controlled Instron machine (USA) with crosshead speed of 1 mm/min at a standard laboratory atmosphere of 23 °C according to ASTM D638. Thickness of the specimens was measured using an electronic dial gauge. The experiment was conducted in five replicates. Fourier transform infrared (FTIR) spectra were obtained using a spectrometer, Nicolet iS5 (USA), connected to an iD5 accessory with a resolution of 4 cm^{-1} averaging 16 scans.

Scanning electron microscope (SEM) images were obtained using Leo Supra 50VP (Germany) equipped with energy dispersive X-ray system. Samples were sputter coated with gold before observation. Transmission electron microscopy (TEM) micrographs were obtained using a Hitachi, H7100 instrument (Japan). Atomic force microscope (AFM) images were captured using Hitachi, AFM5100N (Japan) with scan size of 1 micron at frequency of 0.46 Hz. Preliminary bioactivity of the sample was studied by immersion in SBF solution. Detail preparation of the solution has been reported elsewhere [29]. Sample was immersed in 10 mL of the prepared SBF solution for 7 days to evaluate the growth of hydroxyl apatite (HA). The collected samples were dried and tested for SEM and FTIR.

As for the swelling studies, initial mass of prepared films were weighted. Samples were then immersed in 30 mL of distilled water. Mass of the samples were recorded at predetermined time interval. Swollen films were freed of surface water using filter paper to remove excess water and then weighed. The swelling (%) was calculated using $(W_f - W_i)/W_i \times 100$ in which W_f represent the weight of swollen sample at predetermined time and W_i is the initial weight of the film.

The model drug release experiments were performed at 37˚C in thermostatic orbital shaker (120 rpm). Samples were introduced into 50 mL of phosphate buffer saline (PBS). After predetermined interval, 1 mL of the release medium was collected and another 1 mL of fresh PBS was replaced back into the solution. The release medium was tested using Shimadzu UV-visible spectrometer (Japan) at wavelength of 663 nm to determine the amount of MB released in real time. The percentage of cumulative released was calculated using Eq. 1, in which m_t is the cumulative amount of MB released at time t and m_0 is the total amount of loaded MB.

$$\text{Cumulative release \%} = \frac{m_t}{m_0} \times 100 \qquad (1)$$

3. Results and Discussion

3.1. Tensile Properties

Tensile properties of the κCRG and its nanocomposite films are shown in Fig. 1. Inclusion of mere 1 wt% of HNT to the κCRG film revealed an increased up to nearly 18 and 14 % of the strength and modulus, respectively. It was shown by earlier studies that the addition of non-reinforcing component such as essential oils and fruit extracts reduced the mechanical properties of the CRG film due to the weakening of the network structure [10]. In the present work however, HNT provide reinforcing effects to the κCRG. Higher modulus was attributed to increase in stiffness of the nanocomposite film following the addition of the HNT fillers. The optimum strength and modulus were achieved for nanocomposite films of κCRG/3HNT. This is contributed by the good interaction between the nanotubes with the crosslink structure of the CRG that leads to effective load transfer. High surface area to volume ratios of the HNT resulted in the increased in surface interactions with the κCRG. In comparison with other reported non-tubular clay inclusions to κCRG [12], HNT required lesser loading to achieve its optimum mechanical properties plus with higher strength and modulus values. Furthermore as compared to other 2D nano clays such as montmorillonite, HNT have low surface charges [30]. Thus there will be no intercalation or exfoliation needed to achieve a good dispersion of the nanoclays. The mechanical properties however decreased significantly for samples of κCRG/4HNT. Increasing the HNT content beyond the optimum level had a negative impact on the nanocomposite film. High presence of HNT might disrupt the κCRG crosslink network during gelling. However the strength and modulus of the nanocomposites were still higher than that of the neat κCRG film. This shows that the HNT acted as good reinforcing filler for the κCRG. Elongation at break of the κCRG film was not significantly lowered with the incorporation of HNT at all loading amount, expressing the percentage elongation of the nanocomposite film at fracture was slightly reduced due to increase in rigidity.
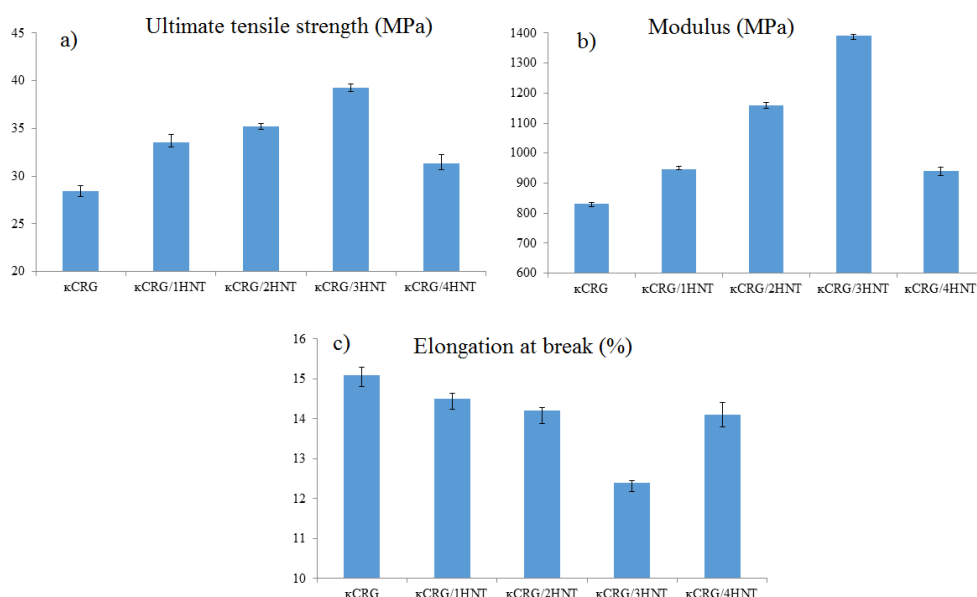
Fig. 1: Tensile properties of κCRG and its nanocomposites:
a) strength b) modulus c) elongation at break

3.2. FTIR Spectroscopy

Figure 2a depicts the typical FTIR spectra of neat κCRG film. The peak at 3345 cm^{-1} can be assigned to the stretching vibration of OH groups, C-H stretching of the CH$_2$ and CH$_3$ groups at 2850-2950 cm^{-1}, C=O stretching at 1643 cm^{-1}, O=S=O stretching at 1224 cm^{-1}, C-O-C stretching at 1158 cm^{-1}, C-O stretching at 1028 cm^{-1}, C-O stretching of the anhydrogalactose at 922 cm^{-1} and C-O-S stretching of the galactose-4-sulfate at 844 cm^{-1} [31]. On the other hand, the incorporation of HNT induced several changes to the vibrational peaks of the κCRG film (Figure 2b). Surface of HNTs composed of siloxane and with hydroxyl groups of silanol, while the inner lumen consists of aluminols. A small peak at 3690 cm^{-1} can be noticeable which represent stretching band of the outer surface of the silanol (Si-OH) of HNT [32]. The absence of any stretching of the hydroxyl groups of aluminol (Al-OH) signifies that the structure of the HNT is still intact in its tubular form while being incorporated within the κCRG. The most significant changes is the disappearance of the C-O-C stretching (1158 cm^{-1}) and the reduction of the C-O-S stretching (844 cm^{-1}) peaks. These can be attributed to the interaction between the κCRG and the HNT components. Shifting of the C-O peaks of anhydrogalactose from 922 to 910 cm^{-1} confirms that the OH groups of κCRG could take part in the hydrogen bond formationwith that group of HNT. In addition, the alumina and silica groups at the HNTs crystal edges facilitate the formation of H bonding between κCRG and HNT. Schematic of the interactions are shown in the insert of Figure 2 (interaction that of glycerol was not shown).
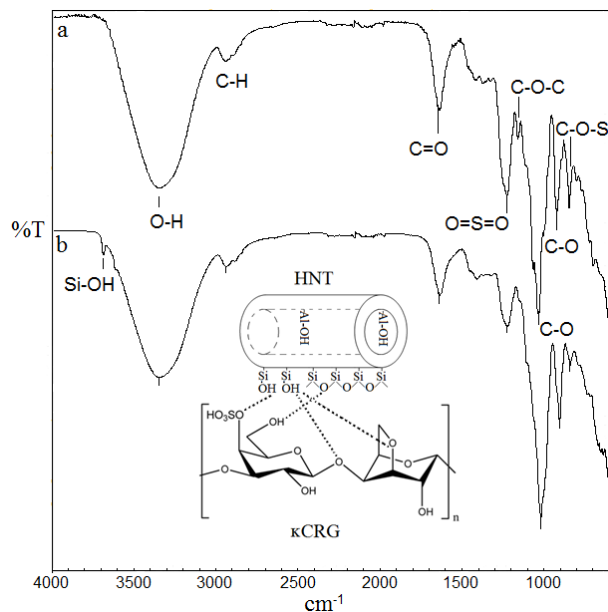
Fig. 2: FTIR spectra of a) neat κCRG and b) κCRG/3HNT

3.3. Morphological and Surface Analysis

Fig. 3a displays the SEM image of the HNT powder. Clear fibrous morphology can be observed. TEM observation of the individual HNT (Figure 3b) revealed the tube-like structure with inner diameter of 21-30 nm and outer diameter of 55-60 nm. Surface of the neat κCRG (Figure 3c) was smooth with good film formation. The 3 wt% of HNT on the other hand induced new surface features to the κCRG. Relatively rough surface can be seen which represent the imbedded HNTs near the film surface. Fine dispersion of the HNTs provides good bonding with the κCRG matrix. No surface cracks or voids were observed. This indicates that the κCRG/3HNT nanocomposite film is intact thus corroborates the mechanical findings of the tensile test. Such uniform HNT morphology would not only increased the mechanical properties but will also provide favorable conditions if the nanocomposite being applied for drug delivery applications. Furthermore the AFM images of κCRG/3HNT (Figure 4b) depict significant changes compared to that of neat κCRG (Fig. 4a). Their average roughness (R_a) and root mean square roughness (R_q) were recorded to be 5.719 and 6.500 nm, respectively. The neat κCRG on the other hand recorded relatively smooth surface with R_a and R_q of 2.111 and 2.491 nm, respectively. The increased of roughness for the nanocomposite film is due to the nanosized clay that induced changes to the surface of the κCRG as observed in accordance to SEM micrograph.
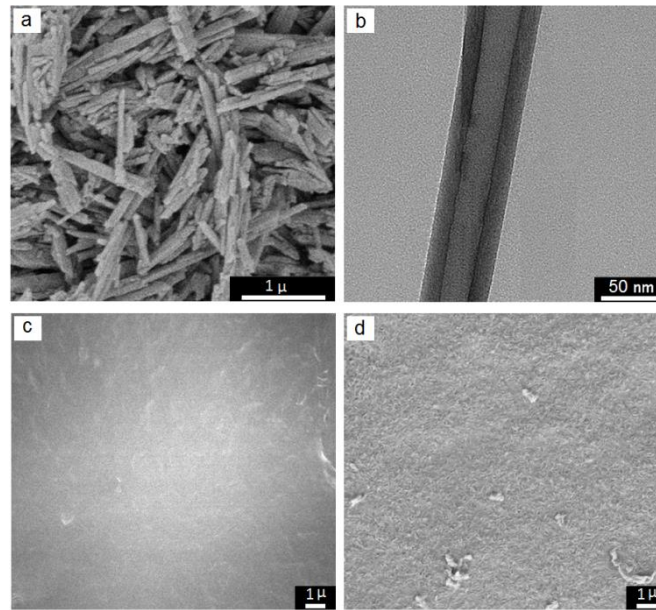
Fig. 3: Electron micrographs of a) HNT powder b) individual HNT c) κCRG d) κCRG/3HNT
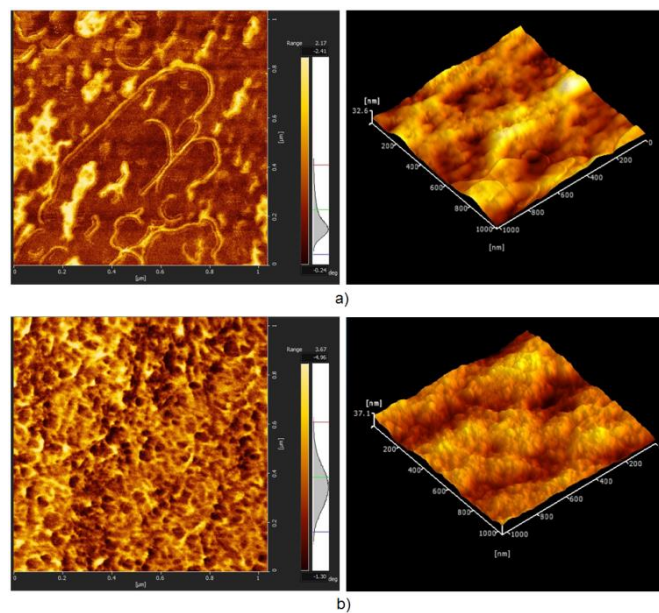

Fig. 4: AFM images of a) κCRG b) κCRG/3HNT

3.4. Growth of Hydroxyl Apatite

The growth of HA by immersion in SBF is a great way to evaluate the bioactivity of the film because the solution composition is very close to that of human blood plasma [33]. SEM images of the κCRG and κCRG/3HNT samples immersed in solution mimicking body fluid for 7 days are shown in Figure 5. Figure 5a revealed small particle that might be that of HA particles formed on the surface of unfilled CRG. It was reported earlier that the hydrophilic sulfonic groups of CRG are exposed on the outside part of the double helix and the hydrophobic domains are exposed on the inside while in physiologic environments [34]. FTIR spectra of the soaked neat κCRG (Figure 6a) indicated that the peaks related to κCRG are still dominant and pronounced. Only the out-of-plane stretching mode of carbonate ions peaks were observed at 1425 and 882 cm^{-1}. This signifies that the surface is still being dominated by the κCRG. It was shown earlier that though crosslink CRG is highly hydrophilic that favors biological compatibility, however the

apatite forming ability of the CRG can be improve by adding other HA enhancing fillers [15]. The nanocomposite film of κCRG/3HNT (Figure 5b) clearly displayed that the surface is being covered by apatite layers. A higher magnification of the surface reveals that the HA coating consisted of porous microstructure formations that were quite similar those of HA on bioactive glass [35]. The resulting FTIR spectra (Fig. 6b) indicated the stretching mode of phosphate ions at 1050, 603 and 574 cm^{-1} and the peaks of carbonate ions that were observed for the κCRG sample. Reduction of the κCRG related vibrations and the significant peaks of HA might suggest that the sample is being deposited by homogenous layers of HA. EDX spectra (Figure 5d) of the soaked CRG/3HNT further corroborates that the observed deposit forms on the film might be of apatite. The Ca/P ratio of the sample was 1.68, a close value to that of adult human bone [36]. The detection of Si suggests that the HNT particles might take a role in the nucleation of HA during the biomimetic process. The presence of silanol groups of HNT induces energetically favorable sites for the Ca to bind onto to form and grow HA nuclei. Furthermore swelling of the CRG film provides such preferable HNT chelating action with the Ca ions. Thus it can be proposed that the swelled κCRG provide the surface functional groups (sulfonic) that induce HA nucleation while the high surface area of HNT (silanol) provide the increase in HA local supersaturation. Schematic of the interactions are depicted in the insert of Figure 6. Though it was shown that other bioactive fillers in CRG such as CaCl [37] and $CaCO_3$ [15] promotes the HA nucleation, mechanical strength of the CRGs are low and longer incubation time needed to form continuous HA layer.
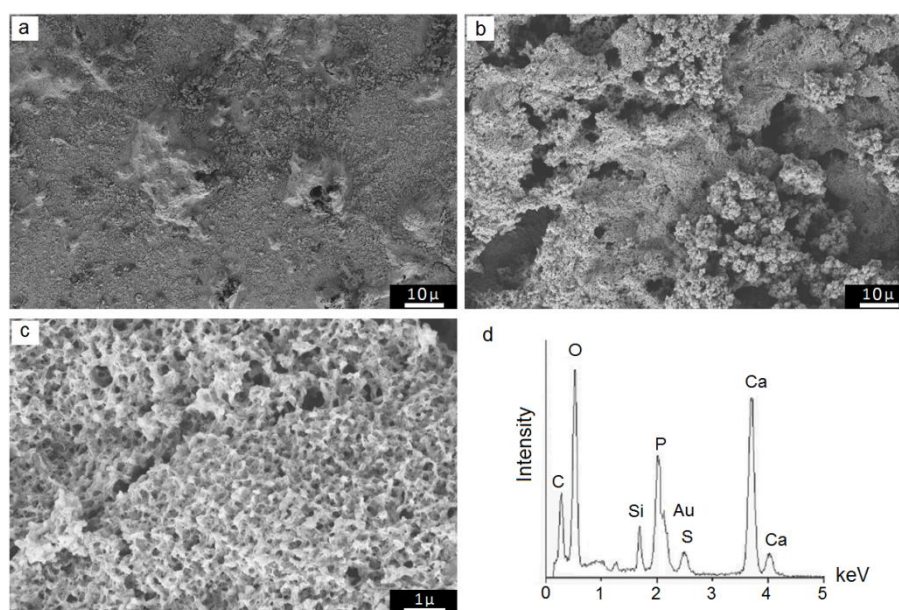

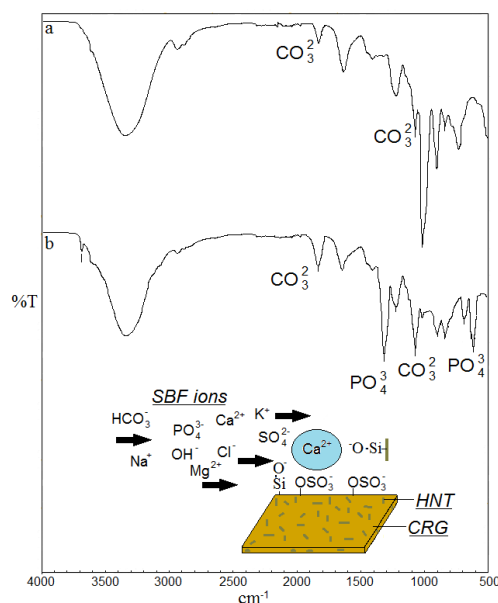*Fig. 5: SEM images of a) κCRG b-c) κCRG/3HNT and d) EDX spectra of κCRG/3HNT after being soaked in SBF for 7 days*

970

Fig. 6: FTIR spectra of a) κCRG b) κCRG/3HNT after being soaked in SBF for 7 days.

3.5. Swelling and Model Drug Release

The swelling of the nanocomposite films provide useful information in drug delivery systems since the hydrogel films exhibit considerable segmental motion that increases the distance between polymer chains. As can be seen in Figure 7a, the neat κCRG swell and rapidly disintegrate after 15 min. The κCRG/3HNT revealed an increased in swelling compared to that of neat κCRG but with much longer disintegration time (>20 min).
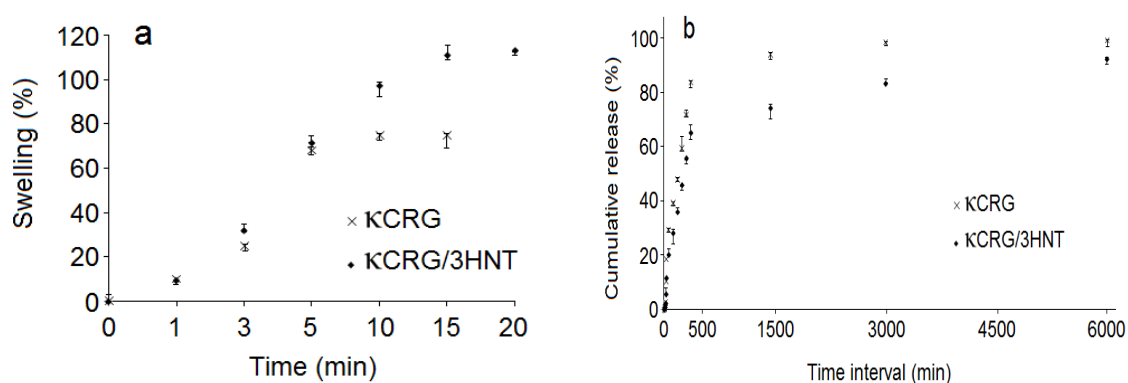

Fig. 7: Swelling and model release of κCRG and κCRG/3HNT.

This behaviour indicates that a more stable structure was obtained by the incorporation of HNTs. On the other hand the increased in swelling is a consequences of the hydrophilicity of the nanotubes that promotes water penetration to the polysaccharide that modifies the chains mobility. The MB release profile of both neat film and nanocomposite film (Figure 7b) revealed initial burst release phenomena [38] and become stable thereafter. The κCRG/3HNT film exhibits delayed release at all time intervals. The incorporation of HNTs seems to slow down the release of MB molecules most probably due to the twisting or distortion of the κCRG matrix. Increased in swelling and delay of MB release profile of the κCRG/3HNT might be due to the effects of HNT that provide hydrophilicity to the matrix and at the same time act as barriers for the release. Swelling and release features of the κCRG/3HNT nanocomposite film could lead to diffusion controlled mechanism for drug delivery.

4. Conclusion

Incorporation of HNT has successfully improved the mechanical, bioactivity and model drug release properties of the κCRG film. The κCRG/3HNT nanocomposite film has the advantages being mechanically reliable for topical drug delivery such as wound healing and favorable bioactivity to support bone tissue regeneration. In addition, cost effective approach utilizing natural resources based on clays and polysaccharide might open up new frontiers in biomedical materials. Nonetheless further investigation is needed to exploit the inner cavities of the HNTs for loading of drug moieties.

References

[1] V. D. Prajapati, P. M. Maheriya, G. K. Jani, H. K. Solanki, Carbohyd. Polym. **105**, 97 (2014).
[2] J. Liu, X. Zhan, J. Wan, Y. Wang, C. Wang, Carbohyd. Polym. **121**, 27 (2015).
[3] A. Pourjavadi, S. Barzegar, F. Zeidabadi, React. Funct. Polym. **67**, 644 (2007).
[4] S. Selvakumaran, I. I. Muhamad, Int. J. Pharm. **496**, 323 (2015).
[5] A. Bani-Jaber, L. Al-Ani, H. Alkhatib, B. Al-Khalidi, AAPS PharmSciTech **12**, 354 (2011).
[6] Y. P. Chao, H. Fu, T. E. Lo, P. T. Chen, J. J. Wang, Biotechnol. Prog. **15**, 1039 (1999).
[7] W. R. Liao, J. Y. Lin, W. Y. Shieh, W. L. Jeng, R. Huang, J. Ind. Microbiol. Biotech. **30**, 433 (2003).
[8] A. K. Dolui, B. Asha, A. Kumar, Indian J. Pharm. Edu. **46**, 70 (2012).
[9] P. Kanmani, J. W. Rhim, Int. J. Biol. Macromol. **68**, 258 (2014).
[10] S. Shojaee-Aliabadi, H. Hosseini, M. A. Mohammadifar, A. Mohammadi, M. Ghasemlou, S. M. Ojagh, R. Khaksar, Int. J. Biol. Macromol. **52**, 116 (2013).
[11] S. Zarina, I. Ahmad, BioResources, **10**, 256 (2015).
[12] J. T. Martins, A. I. Bourbon, A. C. Pinheiro, B. W. Souza, M. A. Cerqueira, A. A. Vicente, Food Bioproc. Tech. **6**, 2081 (2013).
[13] A. R. Ferreira, V. D. Alves, I. M. Coelhoso, Membranes, **6**, 22 (2016).
[14] J. S. Boateng, H. V. Pawar, J. Tetteh, Int. J. Pharm. **441**, 181 (2013).
[15] L. F. Nogueira, B. C. Maniglia, L. S. Pereira, D. R. Tapia- Blácido, A. P. Ramos, Mater. Sci. Eng. C, **58**, 1 (2016).
[16] S. M. Mihaila, E. G. Popa, R. L. Reis, A. P. Marques, M. E. Gomes, Biomacromol. **15**, 2849 (2014).
[17] E. G. Popa, P. P. Carvalho, A. F. Dias, T. C. Santos, V. E. Santo, A. P. Marques, R. L. Reis, J. Biomed. Mater. Res. A **102**, 4087 (2009).
[18] L. Yu, K. Dean, L. Li, Prog. Polym. Sci. **31**, 576(2006).
[19] J. Necas, L. Bartosikova, Vet med-US, **58**, 187 (2013).
[20] J. W. Rhim, J. Food Sci. **77**, N66 (2012).
[21] A. Aldalbahi, P. Feng, Beilstein J. Nanotech. **3**, 415 (2012).
[22] L. R. Rane, N. R. Savadekar, P. G. Kadam, S. T. Mhaske, J. Mater. 2014.
[23] A. L. Daniel da Silva, A. M. Salqueiro, S. Fateixa, J. Moreira, A. C. Estrada, A. M. Gil, T. Trindade, MRS Proceedings, **1403**, 11 (2012).
[24] R. Kamble, M. Ghag, S. Gaikawad, B. K. Panda, J. Adv. Scientific Res. 3 (2012).
[25] M. H. Mousa, Y. Dong, I. J. Davies, Int. J. Polym. Mater. **65**, 225 (2016).
[26] M. Guo, A. Wang, F. Muhammad, W. Qi, H. Ren, Y. Guo, G. Zhu, Chinese J. Chem. **30**, 2115 (2012).
[31] S. R. Levis, P. B Deasy, Int. J. Pharm. **243**, 125 (2002).
[32] A. Molaei, A. Amadeh, M. Yari, M. R. Afshar, Mater. Sci. Eng. C **59**, 740 (2016).
[33] S. I. A. Razak, I. F. Wahab, M. R. A. Kadir, A. Z. M. Khudzari, A. H. M.Yusof, F. N. Dahli, N. H. M. Nayan, T. J. S. Anand, BioResources **11**, 1971 (2016).
[34] D. Rawtani, Y. K. Agrawal, Rev. Adv. Mater. Sci. **30**, 282 (2012)
[35] S. Nanaki, E. Karavas, L. Kalantzi, D. Bikiaris, Carbohyd. Polym. **79**, 1157 (2010)
[36] S. I. A. Razak, N. F. A. Sharif, I. I. Muhamad, Compos. Interface **21**, 715 (2014)
[37] T. Kokubo, H. Takadama, Biomater. **27**, 2907 (2006).

[38] R. Nakata, T. Miyazaki, Y. Morita, E. Ishida, R. Iwatsuki, C. Ohtsuki, J. Ceram. Soc. Jpn. **118**, 487 (2010).

[39] A. Sola, D. Bellucci, V. Cannillo, A. Cattini, Surface Eng. **27**, 560 (2011).

[40] X. Yuan, A. F. Mak, J. Li, J. Biomed. Mater. Res. **57**, 140 (2001).

[41] I. Y. Kim, R. Iwatsuki, K. Kikuta, Y. Morita, T. Miyazaki, C. Ohtsuki, Mater. Sci. Eng. C **31**, 1472 (2011).

[42] H. Hezaveh, I. I. Muhamad, Chem. Eng. Res. Des. **91**, 508 (2013).